potential role of epidermal barrier dysfunction in the pathogenesis of SAK and provide new evidence for its genetic mechanism.

Data availability statement

Datasets related to this article can be found in Table 1.

ORCIDs

Chenmei Liu: http://orcid.org/0000-0002-9724-8162
Chunlei Han: http://orcid.org/0000-0002-2153-7777
Jingyao Liang: http://orcid.org/0000-0001-9635-9162
Chao Yang: http://orcid.org/0000-0002-6598-208X
Youyi Wang: http://orcid.org/0000-0002-4365-2856
Pingjiao Chen: http://orcid.org/0000-0002-3050-8791
Hongyu Chen: http://orcid.org/0000-0002-4885-9717
Hongyan Lu: http://orcid.org/0000-0002-0369-7582
Yan Cai: http://orcid.org/0000-0002-2802-9732
Qi Wang: http://orcid.org/0000-0001-7503-5687
Xibao Zhang: http://orcid.org/0000-0003-1893-4779
Kang Zeng: http://orcid.org/0000-0003-0131-2690
Changxing Li: http://orcid.org/0000-0001-9837-9650

CONFLICT OF INTEREST

The authors state no conflict of interest.

ACKNOWLEDGMENTS

This research was funded by grants from the National Natural Science Foundation of China (NSFC 82173437), the Natural Science Foundation of Guangdong Province (Number 2020A15150875), and the Characteristic Clinic Project of Guangzhou Health Commission (Grant Number 2019TS68).

AUTHOR CONTRIBUTIONS

Conceptualization: CLi; Data Curation: CLiu, YW, QW; Funding Acquisition: CLi; Investigation: CLi, PC, HL; Methodology: HC; Project Administration: CLi, KZ, XZ; Resources: XZ; Software: JL, CY; Supervision: CL; Validation: CL, JL; Writing - Original Draft Preparation: CLiu, CY; Writing - Review and Editing: CLi, CY

Chenmei Liu[1,5], Chunlei Han[2,5], Jingyao Liang[3,5], Chao Yang[4], Youyi Wang[1], Pingjiao Chen[1], Hongyu Chen[1], Hongyan Lu[1], Yan Cai[1], Qi Wang[1], Xibao Zhang[3], Kang Zeng[1] and Changxing Li[1,*]

[1]Department of Dermatology, Nanfang Hospital, Southern Medical University, Guangzhou, China; [2]Department of Dermatology, the Sixth People's Hospital of Dongguan, Dongguan, China; [3]Department of Dermatology, Guangzhou Institute of Dermatology, Guangzhou, China; and [4]Department of Dermatology, Dermatology Hospital, Southern Medical University, Guangzhou, China
[5]These authors contributed equally to this work.
[*]Corresponding author e-mail: lilichangxing@163.com

SUPPLEMENTARY MATERIAL

Supplementary material is linked to the online version of the paper at www.jidonline.org, and at https://doi.org/10.1016/j.jid.2023.01.010.

REFERENCES

Baurecht H, Rühlemann MC, Rodríguez E, Thielking F, Harder I, Erkens AS, et al. Epidermal lipid composition, barrier integrity, and eczematous inflammation are associated with skin microbiome configuration. J Allergy Clin Immunol 2018;141:1668–1676.e16.

Clausen ML, Agner T, Lilje B, Edslev SM, Johannesen TB, Andersen PS. Association of disease severity with skin microbiome and filaggrin gene mutations in adult atopic dermatitis. JAMA Dermatol 2018;154:293–300.

Drislane C, Irvine AD. The role of filaggrin in atopic dermatitis and allergic disease. Ann Allergy Asthma Immunol 2020;124:36–43.

Fan YM, Li SF, Yang YP, Chen QX, Li W. Is acquired symmetrical acrokeratoderma a new dermatosis? Two case reports and Chinese literature review. Int J Dermatol 2010;49:647–52.

Furue K, Ito T, Tsuji G, Ulzii D, Vu YH, Kido-Nakahara M, et al. The IL-13-OVOL1-FLG axis in atopic dermatitis. Immunology 2019;158:281–6.

Kypriotou M, Huber M, Hohl D. The human epidermal differentiation complex: cornified envelope precursors, S100 proteins and the 'fused genes' family. Exp Dermatol 2012;21:643–9.

Li CX, Han CL, Zeng K, Zhang XB, Ma ZL. Clinical, demographic and histopathological features of symmetrical acral keratoderma. Br J Dermatol 2014a;170:948–51.

Li CX, Wen J, Zeng K, Tian X, Li XM, Zhang XB. Ultrastructural study of symmetrical acral keratoderma. Ultrastruct Pathol 2014b;38:420–4.

Liu Z, Zhou Y, Chen RY, Shi G, Li W, Li SJ, et al. Symmetrical acrokeratoderma: a peculiar entity in China? Clinicopathologic and immunopathologic study of 34 new cases. J Am Acad Dermatol 2014;70:533–8.

Salimian J, Salehi Z, Ahmadi A, Emamvirdizadeh A, Davoudi SM, Karimi M, et al. Atopic dermatitis: molecular, cellular, and clinical aspects. Mol Biol Rep 2022;49:3333–48.

Teye K, Numata S, Krol RP, Ishii N, Matsuda M, Lee JB, et al. Prevalence of filaggrin gene mutations in patients with atopic dermatitis and ichthyosis vulgaris in Kyushu area of Japan and South Korea. J Dermatol Sci 2017;86:174–7.

Tsuji G, Hashimoto-Hachiya A, Kiyomatsu-Oda M, Takemura M, Ohno F, Ito T, et al. Aryl hydrocarbon receptor activation restores filaggrin expression via OVOL1 in atopic dermatitis. Cell Death Dis 2017;8:e2931.

Vinay K, Sawatkar GU, Saikia UN, Dogra S. Symmetrical acrokeratoderma: a case series in Indian patients. Orphanet J Rare Dis 2016;11:156.

Yang PP, Peng J, Wu YY, Liu Z, Sheng P, Zhou Y, et al. Immunohistochemical evaluation of epidermal proliferation, differentiation and melanocytic density in symmetrical acrokeratoderma. Clin Exp Dermatol 2017;42:509–15.

GWAs Identify DNA Variants Influencing Eyebrow Thickness Variation in Europeans and Across Continental Populations

Journal of Investigative Dermatology (2023) **143,** 1317–1322; doi:10.1016/j.jid.2022.11.026

TO THE EDITOR

Natural variation in eyebrow thickness (ET) is one of the most conspicuous facial features. Understanding its genetic basis is of broad interest and has implications for dermatology and other

Abbreviations: 1000G, 1000 Genomes; ET, eyebrow thickness; QIMR, Queensland Institute of Medical Research; RS, Rotterdam Study; TZL, Taizhou longitudinal study; US, United States of America

Accepted manuscript published online 20 April 2023

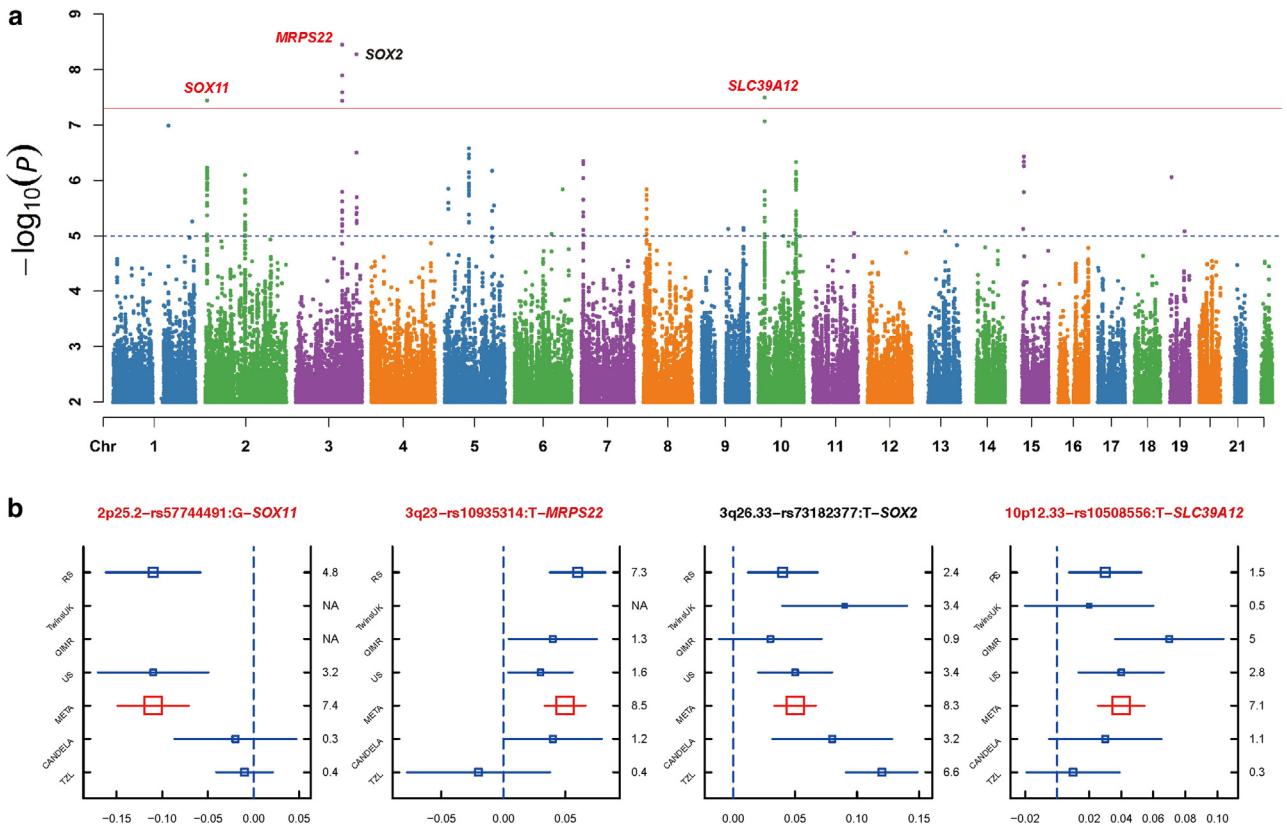

Figure 1. Outcomes of a European GWAS on ET in 9,948 subjects from four cohorts. (**a**) Manhattan plots from a GWAS meta-analysis of four European cohorts (RS, TwinsUK, QIMR, and US). The $-\log_{10}$ *P*-values for association were plotted for each SNP according to its chromosomal position in the human genome assembly GRCh37.p13. Genes previously known from non-European GWASs are indicated in black, whereas previously unreported genes identified in this study in Europeans are in red. The red and blue lines indicate the threshold for genome-wide significant association ($P = 5.00 \times 10^{-8}$) and suggestive association ($P = 1.00 \times 10^{-5}$), respectively. (**b**) Effect sizes for the lead SNPs in the four significantly ET-associated genetic loci 2p25.2-*SOX11*-rs57744491, 3q23-*MRPS22*-rs10935314, 3q26.33-*SOX2*-rs73182377, and 10p12.33-*SLC39A12*-rs10508556. Blue boxes represent linear regression coefficients (x-axis), and red boxes represent effect sizes estimated in the meta-analysis. Horizontal bars indicate a 95% confidence interval of width equal to 1.96 standard errors. The right y-axis indicates *P*-values in each cohort on $-\log_{10}$ scale. META denotes European meta-analysis. Chr, chromosome; ET, eyebrow thickness; QIMR, Queensland Institute of Medical Research; RS, Rotterdam Study; TZL, Taizhou longitudinal study; US, United States of America.

fields. Two GWASs for ET have been reported thus far. In 2,457 Latin Americans from the CANDELA cohort, Adhikari et al. (2016) identified 3q22.3 harboring *FOXL2*. In 2,961 Han Chinese from the Taizhou longitudinal study (TZL) cohort, Wu et al. (2018) discovered 3q26.33 harboring *SOX2* and 5q13.2 harboring *FOXD1* and discovered 2q12.3 harboring *EDAR* by meta-analysis of CANDELA and TZL (Wu et al., 2018). Thus, four ET-associated loci have been established thus far, all in non-Europeans. Because no European ET GWAS had been reported, it remains unknown whether the genetic ET effects described in non-Europeans persist in Europeans or whether there are European-specific genetic loci involved in ET or both.

In this study, we report, to our knowledge, the first GWAS of ET in Europeans using 9,948 individuals from four cohorts of European ancestry, including the Rotterdam Study (RS) (n = 4,441), TwinsUK (n = 1,159, females only), the Queensland Institute of Medical Research (QIMR) study (n = 2,257), and a cohort from the United States of America (US) (n = 2,121) (Supplementary Table S1 and Supplementary Figure S1 and Supplementary Materials and Methods). ET phenotypes were classified from digital facial images into three ordinal levels (thin, intermediate, and thick) (Supplementary Figure S2) as described elsewhere (Wu et al., 2018). Inter-rater concordance was reasonably high (Kappa = 0.34−0.66, Pearson r = 0.51−0.76) (Supplementary Table S2). Increased age, female sex, and blond eyebrow color were significantly associated with thinner eyebrows (Supplementary Table S3 and Supplementary Materials and Methods). Phenotypic correlations between monozygotic twins (TwinsUK $r = 0.75$, QIMR $r = 0.83$) were significantly higher than between dizygotic ones (TwinsUK $r = 0.22$, QIMR $r = 0.35$). Heritability analyses using ACE and ADE models in QIMR twins confirmed a high level of broad sense heritability at 76.27% (69.85−79.79%). Genetic nonadditivity accounted for 28.57% (1.43−59.19%) of variance (dominance), and the additive component (narrow-sense heritability) was 47.70% (18.21−5.16%) (Supplementary Table S4).

GWASs were conducted independently in each of the four cohorts, and the results were meta-analyzed (Figure 1 and Supplementary Figure S3). This European meta-analysis highlighted seven SNPs at four distinct genetic loci showing genome-wide significant ($P < 5 \times 10^{-8}$) ET association, including three previously

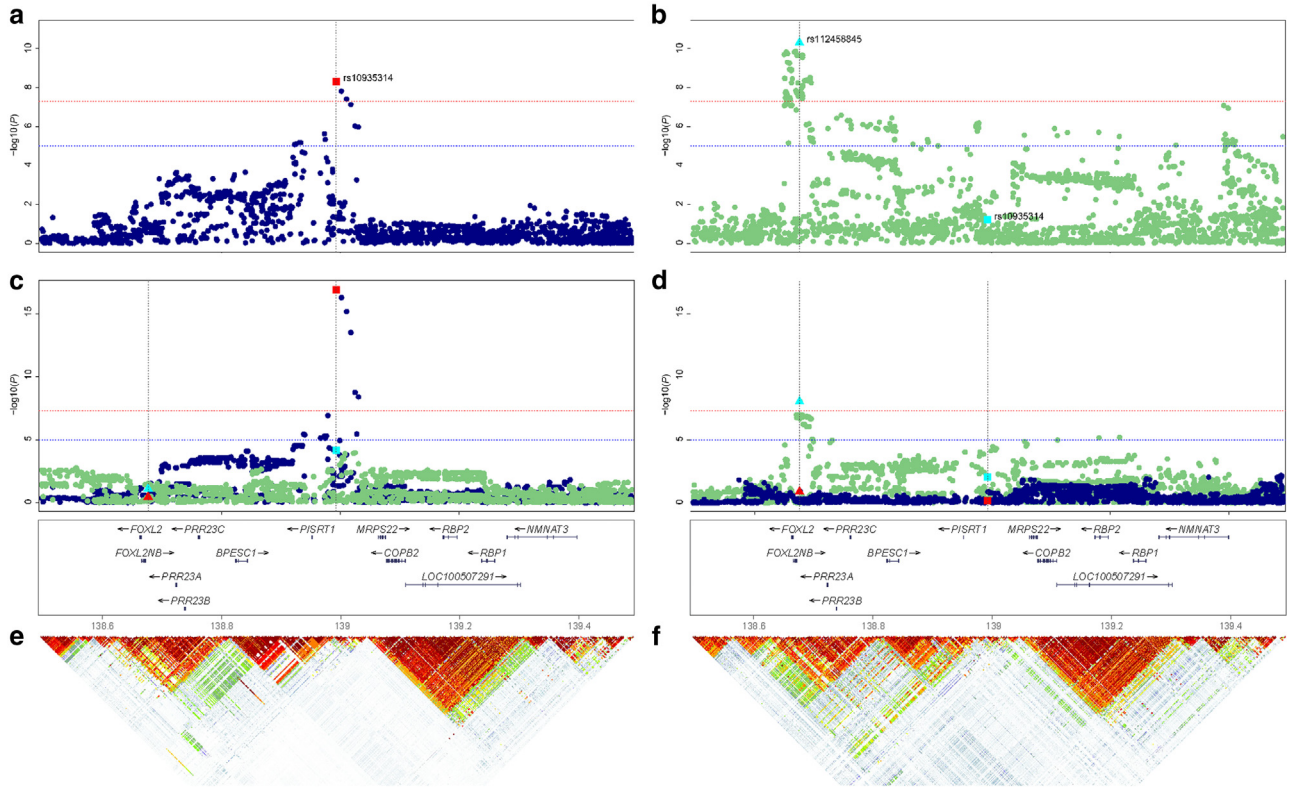

Figure 2. ET association and LD plots for the genetic region harboring 3q23 (*MRPS22*) and 3q22.3 (*FOXL2*). For 3q23, we identified previously unreported ET association in Europeans, whereas for 3q22.3, ET association was previously reported in Latin Americans. Regional association plots for (**a**) European meta-analysis results, (**b**) GWAS results of Latin Americans (CANDELA) as well as simulation results based on (**c**) European and (**d**) Native American population samples from the 1000 Genomes Project. The $-\log_{10}$ *P*-values for eyebrow thickness association were plotted for each SNP according to chromosomal positions (GRCh37.p13). Dark blue dots correspond to the results of Europeans, that is, (**a**) European GWASs (META) and (**c, d**) European population samples from 1000 Genomes (EUR). Light green dots correspond to the results of Americans, that is, (**b**) Latin American GWAS (CANDELA) and (**c, d**) Native American population samples from 1000 Genomes (AMR). The squares and triangles mark the lead SNPs in Europeans (rs10935314) and Latin Americans (rs112458845), respectively. In **c** and **d**, red and cyan colors (for both squares and triangles) correspond to the signals generated in our simulation analyses on the basis of European and Native American population samples from 1000 Genomes, respectively. The gray dashed lines mark the positions of the two lead SNPs in Europeans (rs10935314) and Latin Americans (rs112458845), respectively. The red and blue lines, respectively, correspond to $P = 5 \times 10^{-8}$ and $P = 1 \times 10^{-5}$. (**d, f**) LD plots for (**e**) Europeans (EUR) and (**f**) Native Americans (AMR). META denotes European meta-analysis, EUR denotes European, and AMR denotes Native American. ET, eyebrow thickness; LD, linkage disequilibrium.

unreported loci at 2p25.2 (nearest gene *SOX11*, lead SNP rs57744491, $\beta = -0.11$, $P = 3.60 \times 10^{-8}$), 3q23 (*MRPS22*, rs10935314, $\beta = 0.05$, $P = 3.51 \times 10^{-9}$), and 10p12.33 (*SLC39A12*, rs10508556, $\beta = 0.04$, $P = 3.19 \times 10^{-8}$). The fourth significant locus at 3q26.33 (*SOX2*, rs73182377, $\beta = 0.05$, $P = 5.25 \times 10^{-9}$) (Figure 1 and Supplementary Figure S4 and Supplementary Tables S5 and S6) represents one of the four loci previously discovered in non-Europeans, albeit with a different lead SNP (Wu et al., 2018). The Chinese lead SNP showed a strong but nominally significant association in our European dataset ($P = 3.13 \times 10^{-7}$) (Supplementary Figure S5 and Supplementary Table S6).

The identified locus at 2p25.2 (*SOX11*, rs57744491) was not even nominally significant in the non-Europeans from the CANDELA and TZL cohorts ($P > 0.05$) (Figure 1 and Supplementary Table S6), although the effect was on the same direction across all the six cohorts. This nonsignificant association cannot be explained by allele frequency. The G-allele, increasing ET in Europeans, was sufficiently common in CANDELA and TZL without ET association as well as in other population samples from both continents in the 1000 Genomes (1000G) Project data (1000 Genomes Project Consortium et al., 2015) ($f_{CANDELA} = 0.09$, $f_{TZL} = 0.22$, $f_{AMR1000G} = 0.09$, $f_{EAS1000G} = 0.20$), as it was in Europeans with ET association ($f_{EUR} = 0.05$, missing in TwinsUK and QIMR, $f_{US} = 0.05$, $f_{EUR1000G} = 0.05$). The lead SNP rs57744491 is located ~65 kb upstream of the intron-less gene *SOX11*, which has not been functionally implicated in eyebrow thickness thus far. However, *SOX11* is reported to be a causal gene of the Coffin-Siris syndrome (Coffin-Siris syndrome 9), a congenital multiple malformation syndrome including coarse facial features and hypertrichosis (Tsurusaki et al., 2014), which supports our ET-association findings.

The identified locus at 3q23 (*MRPS22*) is physically close to 3q22.3 (*FOXL2*) previously reported with ET association in CANDELA (Adhikari et al., 2016). The European lead SNP rs10935314 at 3q23 is 317 kb away from the Latin American lead SNP rs112458845 at 3q22.3. The European lead SNP was not even nominally significant ($P > 0.05$) in CANDELA. Large allele frequency differences between Europeans and Americans were seen at rs112458845 ($f_{RS} = 0.003$, non-polymorphic in TwinsUK, QIMR, and

US, $f_{EUR1000G} = 0.002$, $f_{CANDELA} = 0.27$, $f_{AMR1000G} = 0.26$) and at rs10935314 ($f_{RS} = 0.44$, missing in TwinsUK, $f_{QIMR} = 0.45$, $f_{US} = 0.46$, $f_{EUR1000G} = 0.46$, $f_{CANDELA} = 0.26$, $f_{AMR1000G} = 0.25$) (Supplementary Figure S6). These two SNPs fell in different linkage disequilibrium blocks in Europeans and Americans ($r^2_{EUR1000G} = 3.05 \times 10^{-6}$, $r^2_{AMR1000G} = 0.08$) (Figure 2). Simulating genuine effects for these two SNPs on the basis of 1000G data (Figure 2 and Supplementary Materials and Methods) provides additional support for the presence of allelic heterogeneity at the 3q23-3q22.3 region. This likely explains the contrasting association signals at these two different albeit closely spaced genetic loci in different continental populations. A European patient with eyelid ptosis and scarce eyebrows had a 197-kb de novo deletion upstream of *FOXL2*, involving a regulatory element in which our European lead SNP is located (Bertini et al., 2019), which has a prolonged conversion relationship with *FOXL2* (Supplementary Figure S7) in a chromatin interaction analysis with paired-end tag database (Zhou et al., 2013). This finding together with our results suggests a regulatory role of rs10935314 in Europeans, whereas it is absent in non-Europeans, at least in Americans.

At the identified locus 10p12.33, the lead SNP rs10508556 is an intronic variant of *SLC39A12*, which belongs to a subfamily of genes encoding proteins that show structural characteristics of zinc transporters (Taylor and Nicholson, 2003). Functional knowledge of *SLC39A12* in hair development is limited. The T-allele, increasing ET in Europeans, has a high frequency across all relevant groups ($f_{RS} = 0.47$, $f_{TwinsUK} = 0.46$, $f_{QIMR} = 0.48$, $f_{US} = 0.46$, $f_{CANDELA} = 0.63$, $f_{TZL} = 0.73$, $f_{EUR1000G} = 0.44$, $f_{AMR1000G} = 0.63$, $f_{EAS1000G} = 0.69$). The allele effect was in the same direction across all the four European cohorts as well as in CANDELA and TZL (Figure 1 and Supplementary Table S6). The latter might suggest a lack of power in detecting this locus in previous non-European GWASs and strengthens the reliability of our association finding.

Of the four ET-associated loci previously reported in non-Europeans, two, that is, 3q22.3 *FOXL2* and 3q26.33 *SOX2*, have been discussed earlier, whereas 5q13.2 *FOXD1* showed nominally significant association in our European dataset (rs12651896 $P = 5.65 \times 10^{-3}$) (Supplementary Figure S5 and Supplementary Table S6), and 2q12.3 *EDAR* is almost nonpolymorphic in Europeans (rs1866188 $f_{EUR1000G} = 0.01$; $f < 0.01$ in RS, TwinsUK, QIMR, and US) (Supplementary Figure S5 and Supplementary Table S6).

In conclusion, the first GWAS of eyebrow thickness in Europeans discovered three previously unreported genetic loci 2p25.2 *SOX11*, 3q23 *MRPS22*, and 10p12.33 *SLC39A12* with genome-wide significant ET association. Moreover, it rediscovered in Europeans two of the four loci previously found in non-Europeans: 3q26.33 *SOX2* with genome-wide association and 5q13.2 *FOXD1* with nominally significant association. The other two loci previously reported in non-Europeans, 2q12.3 *EDAR* and 3q22.3 *FOXL2*, had no pronounced effects in Europeans, most likely owing to very low allele frequencies. Our study significantly improves the genetic knowledge of human eyebrow variation by increasing the number of known genes from four to seven and delivers previously unreported targets for future functional studies. We show that the phenotypic variation of human eyebrows is determined by both shared and distinct genetic effects across continental populations. Our findings underline the need for studying various population samples of different ancestries for unveiling the genetic basis of human traits, including but not restricted to appearance.

Ethics Statement

Human subjects: All cohort participants gave written informed consent and consent to publish. Ethical approvals were provided for the RS according to the Population Study Act Rotterdam Study (Wet Bevolkingsonderzoek ERGO) executed by the Ministry of Health, Welfare and Sports of The Netherlands, for the TwinsUK study by the St. Thomas' Hospital Local Research Ethics Committee, for the QIMR study by the QIMR Human Research Ethics Committee, and for the US study by the Indiana University Internal Review Board.

Data availability statement

Datasets related to this article regarding the full GWAS summary statistics of eyebrow thickness for the discovery cohorts Rotterdam Study, TwinsUK, Queensland Institute of Medical Research, and United States as well as the meta-analysis of all the four GWASs can be found at figshare with the DOI number 10.6084/m9.figshare.19078070 (https://figshare.com/s/50e489c672fe2d7a9194). The summary statistics of all analyzed DNA variants in the previously published Taizhou longitudinal study and CANDELA GWAS datasets, which were used in this study in addition to the European data, can be found at the National Omics Data Encyclopedia (http://www.biosino.org/node/) under accession number OEZ000393.

ORCIDs

Fuduan Peng: http://orcid.org/0000-0003-4068-530X
Ziyi Xiong: http://orcid.org/0000-0002-2361-2849
Gu Zhu: http://orcid.org/0000-0002-5691-1917
Pirro G. Hysi: http://orcid.org/0000-0001-5752-2510
Ryan J. Eller: http://orcid.org/0000-0002-5632-2792
Sijie Wu: http://orcid.org/0000-0003-4087-4274
Kaustubh Adhikari: http://orcid.org/0000-0001-5825-4191
Yan Chen: http://orcid.org/0000-0002-6873-8648
Yi Li: http://orcid.org/0000-0002-2448-9176
Rolando Gonzalez-José: http://orcid.org/0000-0002-8128-9381
Lavinia Schüler-Faccini: http://orcid.org/0000-0002-2428-0460
Maria-Cátira Bortolini: http://orcid.org/0000-0003-0598-3854
Victor Acuña-Alonzo: http://orcid.org/0000-0003-2205-7625
Samuel Canizales-Quinteros: http://orcid.org/0000-0002-4833-6932
Carla Gallo: http://orcid.org/0000-0001-8348-0473
Giovanni Poletti: http://orcid.org/0000-0001-7576-0301
Gabriel Bedoya: http://orcid.org/0000-0002-4820-6679
Francisco Rothhammer: http://orcid.org/0000-0001-5228-1180
André G. Uitterlinden: http://orcid.org/0000-0002-7276-3387
M. Arfan Ikram: http://orcid.org/0000-0003-0372-8585
Tamar Nijsten: http://orcid.org/0000-0001-9940-2875
Andrés Ruiz-Linares: http://orcid.org/0000-0001-8372-1011
Sijia Wang: http://orcid.org/0000-0001-6961-7867
Susan Walsh: http://orcid.org/0000-0002-7064-1589

Timothy D. Spector: http://orcid.org/0000-0002-9795-0365
Nicholas G. Martin: http://orcid.org/0000-0003-4069-8020
Manfred Kayser: http://orcid.org/0000-0002-4958-847X
Fan Liu: http://orcid.org/0000-0001-9241-8161

CONFLICT OF INTEREST

The authors state no conflict of interest.

ACKNOWLEDGMENTS

The authors gratefully acknowledge all volunteers who participated in the cohort studies. We thank Luba Pardo-Cortes for help in image ascertainment in Rotterdam Study, Kerrie McAloney for data collection at Queensland Institute of Medical Research, and Scott Gordon for data management at Queensland Institute of Medical Research. We are grateful to three anonymous reviewers for their useful comments. FL is supported by the Strategic Priority Research Program of the Chinese Academy of Sciences (XDB38010400) and the National Natural Science Foundation of China (81930056 and 91651507). KA is supported by the Santander Research and Scholarship Award, Bogue Fellowship from University College London. ARL is supported by the Leverhulme Trust (F/07 134/DF), Biotechnology and Biological Sciences Research Council (BB/I021213/1), the Excellence Initiative of Aix-Marseille University - A*MIDEX (a French Investissements d'Avenir programme, 2RUIZLRE/RHRE/ID18HRU201, and 20-07874), the National Natural Science Foundation of China (number 31771393), the Scientific and Technology Committee of Shanghai Municipality (18490750300), the Ministry of Science and Technology of China (2020YFE0201600), the Shanghai Municipal Science and Technology Major Project (2017SHZDZX01), and the 111 Project (B13016). SEM is supported by a National Health and Medical Research Council fellowship (APP1103623). The generation of the GWAS datasets of the Rotterdam Study was supported by the Netherlands Organisation of Scientific Research NWO Investments (175.010.2005.011, 911-03-012); the Genetic Laboratory of the Department of Internal Medicine, Erasmus MC; the Research Institute for Diseases in the Elderly (014-93-015); and The Netherlands Genomics Initiative/Netherlands Organisation for Scientific Research (now) Netherlands Consortium for Healthy Aging (050-060-810). The Rotterdam Study is funded by the Erasmus MC, University Medical Center and the Erasmus University Rotterdam; The Netherlands Organization for the Health Research and Development (ZonMw); the Research Institute for Diseases in the Elderly; the Ministry of Education, Culture and Science; the Ministry for Health, Welfare and Sports; the European Commission (DG XII); and the Municipality of Rotterdam. The TwinsUK study is funded by the Wellcome Trust, the Medical Research Council, the European Union (FP7/2007-2013), the National Institute for Health Research–funded BioResource, and the Clinical Research Facility and Biomedical Research Centre based at Guy's and St Thomas' NHS Foundation Trust in partnership with King's College London. Queensland Institute of Medical Research acknowledges funding by the Australian National Health and Medical Research Council (241944, 339462, 389927, 389875, 389891, 389892, 389938, 442915, 442981, 496739, 552485, 552498) and the Australian Research Council (A7960034, A79906588, A79801419, DP0770096, DP0212016, DP0343921) for building and maintaining the adolescent twin family resource through which samples were collected. All information and work pertaining to the United States cohort were generated under funding by the United States National Institute of Justice (2014-DNBX-K031) to SWal.

AUTHOR CONTRIBUTIONS

Conceptualization: FL, MK, NGM, TDS, SWal; Data Curation: FP, ZX, GZ, PGH, RJE, SWu, KA; Formal Analysis: FP, ZX, GZ, PGH, RJE, SWu, KA, YC, YL; Funding Acquisition: RGJ, LSF, MCB, VAA, SCQ, CG, GP, GB, FR, AGU, MAI, TN, ARL, SWan, SWal, TDS, NGM, MK, FL; Resources: RGJ, LSF, MCB, VAA, SCQ, CG, GP, GB, FR, AGU, MAI, TN, ARL, SWan, SWal, TDS, NGM, MK, FL; Supervision: ARL, SWan, SWal, TDS, NGM, MK, FL; Writing – Original Draft Preparation: FL, FP, MK; Writing – Review and Editing: FP, ZX, GZ, PGH, RJE, SWu, KA, YC, YL, RGJ, LSF, MCB, VAA, SCQ, CG, GP, GB, FR, AGU, MAI, TN, ARL, SWan, SWal, TDS, NGM, MK, FL

Disclaimer

None of the funders had any influence on this study.

Fuduan Peng[1,2,3], Ziyi Xiong[4,5], Gu Zhu[6], Pirro G. Hysi[7], Ryan J. Eller[8], Sijie Wu[9], Kaustubh Adhikari[10,11,12], Yan Chen[1,2,4,13], Yi Li[1,2,13], Rolando Gonzalez-José[14], Lavinia Schüler-Faccini[15], Maria-Cátira Bortolini[16], Victor Acuña-Alonzo[16], Samuel Canizales-Quinteros[17], Carla Gallo[18], Giovanni Poletti[18], Gabriel Bedoya[19], Francisco Rothhammer[20], André G. Uitterlinden[5,21], M. Arfan Ikram[5], Tamar Nijsten[22], Andrés Ruiz-Linares[10,23,24], Sijia Wang[9,25,26,27], Susan Walsh[8], Timothy D. Spector[7], Nicholas G. Martin[6], Manfred Kayser[4,28,*] and Fan Liu[1,2,4,13,28]; on behalf of the International Visible Trait Genetics (VisiGen) Consortium

[1]CAS Key Laboratory of Genomic and Precision Medicine, Beijing Institute of Genomics, Chinese Academy of Sciences, Beijing, China; [2]University of Chinese Academy of Sciences, Beijing, China; [3]Department of Genomic Medicine, The University of Texas MD Anderson Cancer Center, Houston, Texas, USA; [4]Department of Genetic Identification, Erasmus MC, University Medical Center Rotterdam, Rotterdam, The Netherlands; [5]Department of Epidemiology, Erasmus MC, University Medical Center Rotterdam, Rotterdam, The Netherlands; [6]QIMR Berghofer Medical Research Institute, Brisbane, Australia; [7]Department of Twin Research & Genetic Epidemiology, School of Life Course & Population Sciences, King's College London, London, United Kingdom; [8]Department of Biology, School of Science, Indiana University-Purdue University Indianapolis, Indianapolis, Indiana, USA; [9]CAS Key Laboratory of Computational Biology, CAS-MPG Partner Institute for Computational Biology, Shanghai Institute of Nutrition and Health, Shanghai Institutes for Biological Sciences, University of Chinese Academy of Sciences, Chinese Academy of Sciences, Shanghai, China; [10]Department of Genetics, Evolution and Environment, Division of Biosciences, London, United Kingdom; [11]Genetics Institute, Division of Biosciences, University College London, London, United Kingdom; [12]School of Mathematics & Statistics, Faculty of Science, Technology, Engineering & Mathematics, The Open University, Milton Keynes, United Kingdom; [13]China National Center for Bioinformation, Beijing, China; [14]Instituto Patagónico de Ciencias Sociales y Humanas, Centro Nacional Patagónico, Consejo Nacional de Investigaciones Científicas y Técnicas (CONICET), Puerto Madryn, Argentina; [15]Departamento de Genética, Universidade Federal do Rio Grande do Sul, Porto Alegre, Brasil; [16]Molecular Genetics Laboratory, National School of Anthropology and History, Mexico City, Mexico; [17]Unidad de Genomica de Poblaciones Aplicada a la Salud, Facultad de Química, Universidad Nacional Autónoma de México (UNAM)-Instituto Nacional de Medicina Genómica, Mexico City, Mexico; [18]Laboratorios de Investigación y Desarrollo, Facultad de Ciencias y Filosofía, Universidad Peruana Cayetano Heredia, Lima, Perú; [19]GENMOL (Genética Molecular), Universidad de Antioquia, Medellín, Colombia; [20]Instituto de Alta Investigación, Universidad de Tarapacá, Arica, Chile; [21]Department of Internal Medicine, Erasmus MC, University Medical Center Rotterdam, Rotterdam, The Netherlands; [22]Department of Dermatology, Erasmus MC, University Medical Center Rotterdam, Rotterdam, The Netherlands; [23]CNRS, EFS, ADES UMR 7268, Faculté de Médecine Timone, Aix-Marseille Université, Marseille, France; [24]Ministry of Education Key Laboratory of Contemporary Anthropology and Collaborative Innovation Center of Genetics and Development, School of Life Sciences and Human Phenome Institute, Fudan University, Shanghai, China; [25]State Key Laboratory of Genetic Engineering and Ministry of Education Key Laboratory of Contemporary Anthropology, Collaborative Innovation Center for Genetics and Development, School of Life Sciences, Fudan University, Shanghai, China; [26]Human Phenome Institute, Fudan University, Shanghai, China; and [27]Center for Excellence in Animal Evolution and Genetics, Chinese Academy of Sciences, Kunming, China
[28]These authors contributed equally to this work.
[*]Corresponding author e-mail: m.kayser@erasmusmc.nl

SUPPLEMENTARY MATERIAL

Supplementary material is linked to the online version of the paper at www.jidonline.org, and at https://doi.org/10.1016/j.jid.2022.11.026.

REFERENCES

1000 Genomes Project Consortium, Auton A, Brooks LD, Durbin RM, Garrison EP, Kang HM, et al. A global reference for human genetic variation. Nature 2015;526:68–74.

Adhikari K, Fontanil T, Cal S, Mendoza-Revilla J, Fuentes-Guajardo M, Chacón-Duque JC, et al. A genome-wide association scan in admixed Latin Americans identifies loci influencing facial and scalp hair features. Nat Commun 2016;7:10815.

Bertini V, Valetto A, Baldinotti F, Azzarà A, Cambi F, Toschi B, et al. Blepharophimosis, Ptosis, Epicanthus Inversus syndrome: new report with a 197-kb deletion upstream of FOXL2 and review of the literature. Mol Syndromol 2019;10:147–53.

Taylor KM, Nicholson RI. The LZT proteins; the LIV-1 subfamily of zinc transporters. Biochim Biophys Acta 2003;1611:16–30.

Tsurusaki Y, Koshimizu E, Ohashi H, Phadke S, Kou I, Shiina M, et al. De novo SOX11 mutations cause Coffin-Siris syndrome. Nat Commun 2014;5:4011.

Wu S, Zhang M, Yang X, Peng F, Zhang J, Tan J, et al. Genome-wide association studies and CRISPR/Cas9-mediated gene editing identify regulatory variants influencing eyebrow thickness in humans. PLoS Genet 2018;14:e1007640.

Zhou X, Lowdon RF, Li D, Lawson HA, Madden PA, Costello JF, et al. Exploring long-range genome interactions using the WashU epigenome Browser. Nat Methods 2013;10:375–6.

Proteasome Inhibitors Interact Synergistically with BCL2, Histone Deacetylase, BET, and Jak Inhibitors against Cutaneous T-Cell Lymphoma Cells

Journal of Investigative Dermatology (2023) **143,** 1322–1325; doi:10.1016/j.jid.2022.12.017

TO THE EDITOR

Cutaneous T-cell lymphoma (CTCL) is often refractory to treatment at advanced stages with blood involvement (Dummer et al., 2021). We have previously revealed the synergistic cytotoxic effects of inhibiting BCL2, histone deacetylase, BET, and/or Jak in patient-derived CTCL cells and CTCL cell lines, suggesting potential advantages of a spectrum of combination treatment strategies for this disease (Cyrenne et al., 2017; Kim et al., 2018; Yumeen et al., 2020). Proteasome inhibitors target multiple pathways, including protein degradation, to cause cytotoxicity and have been utilized in other hematologic malignancies. They have shown efficacy as a single agent in a small phase II trial of patients with relapsed or refractory CTCL (Zinzani et al., 2007) as well as in limited combinations during preclinical studies (Yumeen et al., 2020) and early clinical trials (Holkova et al., 2017). In this study, we share our expanded preclinical assessment of the synergistic activity of proteasome inhibitors when used with the BCL2 inhibitor venetoclax, histone deacetylase inhibitor vorinostat, BET inhibitor mivebresib, or Jak inhibitor fedratinib. We reveal that the cytotoxic effects from combination treatment were greater than additive when assessed in patient-derived CTCL cells. Furthermore, we show an increase in apoptosis pathway activation with combination treatment and explore the gene expression changes underlying these synergistic effects.

Nine patients with CTCL provided written informed consent at Yale Cancer Center (New Haven, CT) in accordance with the Yale Human Investigational Review Board (Table 1). Malignant cells were isolated from peripheral blood as previously described (Kim et al., 2018). HH and HUT78 cells were procured from ATCC (Manassas, VA), and MyLa 2059 was provided by E. Contassot (University Hospital Zurich, Zurich, Switzerland). We have previously characterized the genetic alterations in HH and HUT78 (Lin et al., 2012). Cell lines tested negative for *Mycoplasma* contamination by PCR. Seventy-two-hour cell viability assays were conducted as previously described (Kim et al., 2018). The degree of synergy was quantified as a combination index using the Chou-Talalay method (Chou, 2010). For caspase-mediated apoptosis studies, primary cells were incubated for 48 hours with 0.0167 μM of oprozomib and approximately three-fold of the 50% inhibitory concentration of the second drug. Caspase-Glo 3/7 (Promega, Madison, WI) was used to measure caspase activity. Gene expression profiling was performed as previously described (Kim et al., 2018). Statistical analysis was performed using GraphPad Prism, version 9.4.0 (GraphPad Software, San Diego, CA).

Primary CTCL cells from seven patients and three CTCL cell lines (HH, MyLa, and HUT78) were treated with the following proteasome inhibitors in cell viability assays: first-generation bortezomib and second-generation oprozomib, ixazomib, carfilzomib, and marizomib (Figure 1a). We found that both primary CTCL cells and cell lines were highly sensitive to the inhibitors with mean 50% inhibitory concentration values in the nanomolar range, the most potent being carfilzomib and the least being marizomib. All proteasome inhibitors except for marizomib showed significantly lower 50% inhibitory concentration values against CTCL cells than against normal CD4+ T cells isolated from healthy controls (Supplementary Table S1). For combination treatment testing, we selected bortezomib for being first of

Abbreviations: CTCL, cutaneous T-cell lymphoma; UPR, unfolded protein response

Accepted manuscript published online 13 January 2023; corrected proof published online 12 February 2023

SUPPLEMENTARY MATERIALS AND METHODS

Rotterdam Study

The **Rotterdam Study** (RS) is a population-based prospective study of 14,926 participants aged ≥45 years living in a suburb of Rotterdam, The Netherlands. Details regarding the cohort profile have been described previously (Hofman et al., 2015). A total of 5,604 participants not wearing make-up, cream, or jewelry were photographed using a Premier 3dMD face3-plus UHD camera (3dMD, Atlanta, GA). Frontal two-dimensional portrait photos were projected from the three-dimensional images and were used for eyebrow phenotyping. The RS has been approved by the medical ethics committee according to the Wet Bevolkingsonderzoek ERGO (Population Study Act Rotterdam Study) and executed by the Ministry of Health, Welfare and Sports of The Netherlands. All participants provided written informed consent. Genotyping was carried out using the Infinium II HumanHap 550K Genotyping BeadChip, version 3 (Illumina, San Diego, CA). Collection and purification of DNA have been described previously (Kayser et al., 2008). All SNPs were imputed using MACH software (www.sph.umich.edu/csg/abecasis/MaCH/) on the basis of the 1000-Genomes Project reference population information (1000 Genomes Project Consortium et al., 2012). Genotype and individual quality controls (QCs) have been described in detail previously (Lango Allen et al., 2010). After all QCs, this study included a total of 6,886,438 autosomal SNPs and 4,411 individuals.

TwinsUK Study

The TwinsUK study included 3,347 female participants of European origin within the TwinsUK adult twin registry based at St. Thomas' Hospital (London, United Kingdom). All participants gave fully informed consent under a protocol reviewed by the St. Thomas' Hospital Local Research Ethics Committee. This study includes 1,574 participants for whom high-resolution 3dMDface digital photographs were taken. Frontal two-dimensional portrait photos were generated using three-dimensional images and were used for eyebrow phenotyping. Genotyping of the TwinsUK cohort was done with a combination of Illumina HumanHap300 and HumanHap610Q chips. Intensity data for each of the arrays were pooled separately, and genotypes were called with the Illuminus32 calling algorithm, thresholding on a maximum posterior probability of 0.95 as previously described (Small et al., 2011). Imputation was performed using the IMPUTE 2.0 software package using haplotype information from the 1000-Genomes Project (phase 1, integrated variant set across 1,092 individuals, version 2, March 2012). SNPs with minor allele frequency (MAF) < 5%, overall call rate <97%, and Hardy–Weinberg equilibrium $P <$ 1e-4 were removed. After all QCs, this study included a total of 4,699,858 autosomal SNPs and 1,159 women.

Queensland Institute of Medical Research study

Participants were genotyped on the Illumina Human610-Quad and Core + Exome SNP chips. These samples were genotyped in the context of a larger genome-wide association project that resulted in the genotyping of 28,028 individuals using the Illumina 317, 370, 610, 660, Core + Exome, PsychChip, Omni2.5, and OmniExpress SNP chips, which included data from twins, their siblings, and their parents. Because these samples were genotyped in the context of a larger project, the data were integrated with the larger Queensland Institute of Medical Research (QIMR) genotype project, and the data were checked for pedigree, sex, and Mendelian errors and for non-European ancestry. Because the QIMR genotyping project included data from the multiple chip sets, to avoid introducing bias to the imputed data, individuals genotyped on the Human Hap Illumina chips (the 317, 370, 610, 660K chips) were imputed separately from those genotyped on the Omni chips (the Core+Exome, PsychChip, Omni2.5, and OmniExpress chips). Individuals were imputed to the Haplotype Reference Consortium (HRC.1.1) using a set of SNPs common to the first-generation genotyping platforms (n = ~ 278,000). Imputation was performed on the Michigan Imputation Server using the SHAPEIT/minimac Pipeline. Genotype data were screened for genotyping quality (GenCall < 0.7), SNP and individual call rate (0.95), Hardy–Weinberg equilibrium test (1e-6), and MAF (0.01). After genotype QCs, data were available for 7,624,941 SNPs. This study included 2,404 adolescent twins and singletons for whom two-dimensional portrait photos were taken from a distance of 1–2 meters for identification, with no specific instructions for facial expression. All participants and, where appropriate, their parents or guardians gave informed consent. This study was approved by the QIMR Berghofer Human Research Ethics Committee.

United States study

This cohort is comprised of 3,528 individuals from diverse sampling locations, collected in the United States of America (US), Ireland, and Lebanon. All participants gave informed consent under a protocol reviewed by the Indiana University Internal Review Board. Genotyping was performed using the Infinium Multi-Ethnic Global BeadChip array on an Illumina Hiseq (Illumina) from DNA that had been extracted and purified from participant saliva samples using an in-house salting out method. Pre-imputation QCs involved filtering out poorly genotyped variants (SNP-wise call rate < 0.95, Hardy–Weinberg equilibrium $P <$ 1e-6, and MAF < 0.025) and individuals (call rate < 0.9). All variants were phased and imputed using SHAPEIT (Delaneau et al., 2011) and IMPUTE (Bycroft et al., 2017[1]; Marchini et al., 2007), respectively. The 1000-Genomes Project (International HapMap Consortium, 2003) reference panel and the Haplotype Research Consortium (1000 Genomes Project Consortium et al., 2012) reference panel were merged through cross-imputation in IMPUTE and then used as the reference panel for imputation. Postimputation QCs involved filtering out related individuals (identity by descent > 0.1875) and variants that had low imputation confidence (information score reported by IMPUTE < 0.3). Owing to the diverse sampling locations, genomic admixture was accessed to remove individuals of

[1] Bycroft C, Freeman C, Petkova D, Band G, Elliott LT, Sharp K, et al. Genome-wide genetic data on ~ 500,000 UK Biobank participants. bioRxiv 2017.

non-European descent using an Eigensoft-like exclusion method. Specifically, using European reference samples from the 1000-Genomes Project (Genomes Project et al., 2015) and the Human Genome Diversity Project (Cann et al., 2002) retrieved from http://hagsc.org/hgdp/files.html, a European centroid was calculated from eigenvectors calculated from a principal component analysis. Study individuals falling outside of three SDs of this European centroid on six dimensions were excluded. After all QCs, this study included 2,121 individuals and 6,165,244 SNPs.

Details regarding sample characteristics, phenotyping, genotyping, and GWAS in CANDELA and Taizhou longitudinal study have been described previously (Adhikari et al., 2016; Wu et al., 2018). GWAS data in all cohorts were aligned according to human reference assembly GRCh37.p13.

Genotype QC

As described earlier, genotype QC was independently conducted in each cohort with slightly different QC parameters (Supplementary Table S7). All SNPs in all cohorts passed these lower-bound QC parameters, that is, SNP-wise call rate (0.95), Hardy–Weinberg equilibrium test (1e-4), MAF (0.01), and identity by descent (0.2). In addition, SNPs that were missing in more than two cohorts were removed. Genomic relatedness matrix was derived for RS and US using GCTA (genome-wide complex trait analysis) (Yang et al., 2011), where no individuals were identified as close relatives (identity by descent $>$ 0.1). Genomic principal component analysis was performed for all four cohorts together with 2,504 samples from the 1000-Genomes Project, where all individuals were clustered together with the European samples from the 1000-Genomes Project. After all QCs, a total of 6,370,473 SNPs were available for the subsequent analysis.

Computer simulations

We conducted a simulation analysis to examine whether allelic heterogeneity at 3q23-3q22.3 may explain the different associations observed between Europeans and Latin Americans. Phenotypes were simulated on the basis of real genotypes of Europeans and Native Americans in the 1000-Genomes Project reference panel, assuming a genuine effect for the regional lead SNP in Europeans (rs10935314) or for the lead SNP in Latin Americans (rs112458845).

Consider a linear regression model as follows:

$$y = 1_n\mu + x\beta + \epsilon \text{ with } V = \beta^2 x^T x + \sigma_\epsilon^2$$

where y_i is the phenotype of the i_{th} individual, 1_n is an n-dimensional vector of ones, μ is the general mean, and x_i is the number of the effect allele. The β is the allele effect, and ε is an n-dimensional vector of normally distributed residuals $N(0,\sigma_\varepsilon^2)$. V, the variance of y, is given as a linear combination of the genetic component $x^T x$ and the residual component σ_ε^2. The allele effect is derived as $\beta = \pm\sqrt{\frac{P\sigma_\varepsilon^2}{(1-P)x^T x}}$, where the parameter P (ranging from 0.1 to 0.9) is used to control for the significance level under different sample sizes (European n = 503 and Native Americans n = 263). Because the sample sizes are small, we simulated a large effect to manifest the association significance, that is, y is simulated in such a way that 10% of its variance is explained by the SNP under investigation. Regional association analysis of the simulated phenotypes was carried out separately in Europeans and Native Americans. The resultant patterns of association signals in Europeans and Native Americans were compared with the patterns observed in our Europeans and Latin Americans.

In this region, the patterns of the association signals in our Europeans and Latin Americans (CANDELA) were highly consistent with the simulation results we obtained in Europeans and Native Americans (Figure 2), although the Native Americans–CANDELA comparison is not completely fair because Latin Americans are only partially of Native American ancestry. The fact that simulating a genuine effect for the European-specific SNP or the Latin American–specific SNP resembled the association patterns observed in our Europeans and those observed in CANDELA supports the presence of heterogeneity in this genomic region.

GWAS and meta-analysis

GWASs for eyebrow thickness were independently carried out in RS, TwinsUK, QIMR, and US. GWASs in RS and US (no close relatives) were conducted on the basis of linear models assuming an additive allele effect adjusted for covariates, including sex, age, eyebrow color, and top four genomic principal components using PLINK (Purcell et al., 2007). For GWASs in TwinsUK and QIMR, which contains twins, we used the exact linear mixed model implemented in GEMMA (Zhou and Stephens, 2012) to adjust for family relatedness in addition to the covariates mentioned earlier. The kinship matrix was estimated internally in GEMMA using the 50,000 SNPs we selected from a larger set of linkage disequilibrium pruned ($r^2 < 0.2$) and high frequency (MAF > 0.3) SNPs in European samples from the 1000-Genomes Project. Kinship measures were then used within the linear mixed model framework to structure the variance/covariance matrix of the genetic random effect. A permutation analysis ($k = 10$) in TwinsUK confirmed that the genome-wide type-I error was properly controlled because the genomic inflation factors were all very close to 1.0. Inverse variance fixed-effect meta-analyses were carried out using PLINK to combine GWAS results. *P*-values smaller than 5×10^{-8} were considered to be genome-wide significant. GWAS results were visualized using Manhattan plots and Q–Q plots. Regional Manhattan plots were produced using LocusZoom (Pruim et al., 2010). Allele frequency distribution in 2,504 subjects from the 1000-Genomes Project was visualized using MapViewer.

Eyebrow thickness phenotyping and QC

Eyebrow thickness was assessed on three ordinal levels (thin, intermediate, and thick) by 3–4 raters using a previously proposed protocol (Wu et al., 2018). Images with obvious eyebrow threading/plucking/coloring were removed. In RS, individuals who answered yes to our questionnaires regarding eyebrow threading/plucking/coloring were removed. Each cohort prepared its own reference photos for eyebrow classification. The reference photos in RS are provided (Supplementary Figure S2). Before grading, 3–4 raters were trained using 50 randomly selected photos in comparison with the reference photos to

reach a consensus. After grading, concordance between the raters was evaluated using Pearson correlation coefficients and Kappa's statistic. The average score of all raters was considered numeric in regression analyses.

Inter-rater (for CANDELA, intra-rater) reliability was reasonably high in all cohorts (Kappa = 0.34−0.66, Pearson $r = 0.51-0.76$). Besides, the inter-rater results in all the four newly involved cohorts were reasonably concordant (mean Pearson $r = 0.71$, mean Kappa $K = 0.54$ for RS; mean $r = 0.70$, $K = 0.57$ for TwinsUK; mean $r = 0.73$, mean $K = 0.60$ for QIMR; and mean $r = 0.54$, mean $K = 0.38$ for US) (Supplementary Table S2).

Consistent with the findings in Wu et al. (2018), the female sex ($\beta = -0.38$, $P = 4.10 \times 10^{-106}$ in RS; samples were all female in TwinsUK; $\beta = -0.32$, $P = 6.03 \times 10^{-44}$ in QIMR; $\beta = -0.23$, $P = 3.80 \times 10^{-27}$ in US) showed a significant eyebrow thinning effect (Supplementary Table S3). The phenotypic variance in males was consistently larger than in females (Supplementary Table S8). Whether this is because of more non-natural eyebrow thickness in women than in men for instance (whereas we did exclude obvious cases of non-natural eyebrow shape before analysis) we cannot know. Considering that our cohorts include individuals both young (QIMR), young to middle-aged individuals (US), and elder people (RS and TwinsUK), which all showed similar phenotypic variance differences between males and females, maybe this finding represents natural variation differences between men and women as may be explained by sex-biased selection on human appearance traits, which we believe is beyond the scope of our study. What matters most for our GWAS are genetic effects. We conducted a sex-stratified analysis for the lead SNPs in the RS cohort where we have individual-level data. We found that the allele effects were in the same direction for both sexes. Indeed, the effect sizes were larger in males than in females (Supplementary Table S9), which is consistent with the observation that phenotypic variance was larger in males than in females. we added these results in our revised Supplementary Materials and Methods. Age also showed significantly reduced eyebrow thickness association in both RS ($\beta = -0.01$, $P = 1.33 \times 10^{-10}$), TwinsUK ($\beta = -0.01$, $P = 3.60 \times 10^{-13}$), and US ($\beta = -0.01$, $P = 1.09 \times 10^{-31}$) but not in QIMR ($\beta = 0.02$, $P = 0.14$), which might be explained by only adolescents with similar age being included in QIMR (mean age of 16.43 ± 0.80 years). Darker eyebrows showed significant ($\beta = 0.30$, $P = 1.57 \times 10^{-59}$ in RS; $\beta = 0.44$, $P = 4.65 \times 10^{-34}$ in TwinsUK; $\beta = 0.29$, $P = 2.61 \times 10^{-66}$ in QIMR; $\beta = 0.06$, $P = 1.45 \times 10^{-5}$ in US) eyebrow thickening effect. Because this may likely be explained by a biased perception of the raters (Supplementary Table S3), we adjusted eyebrow color in all GWASs of European descent.

SUPPLEMENTARY REFERENCES

1000 Genomes Project Consortium, Abecasis GR, Auton A, Brooks LD, DePristo MA, Durbin RM, et al. An integrated map of genetic variation from 1,092 human genomes. Nature 2012;491:56−65.

1000 Genomes Project Consortium, Auton A, Brooks LD, Durbin RM, Garrison EP, Kang HM, et al. A global reference for human genetic variation. Nature 2015;526:68−74.

Adhikari K, Fontanil T, Cal S, Mendoza-Revilla J, Fuentes-Guajardo M, Chacón-Duque JC, et al. A genome-wide association scan in admixed Latin Americans identifies loci influencing facial and scalp hair features. Nat Commun 2016;7:10815.

Cann HM, de Toma C, Cazes L, Legrand MF, Morel V, Piouffre L, et al. A human genome diversity cell line panel. Science 2002;296:261−2.

Delaneau O, Marchini J, Zagury JF. A linear complexity phasing method for thousands of genomes. Nat Methods 2011;9:179−81.

Hofman A, Brusselle GG, Darwish Murad S, van Duijn CM, Franco OH, Goedegebure A, et al. The Rotterdam Study: 2016 objectives and design update. Eur J Epidemiol 2015;30:661−708.

International HapMap Consortium. The international HapMap project. Nature 2003;426:789−96.

Kayser M, Liu F, Janssens AC, Rivadeneira F, Lao O, van Duijn K, et al. Three genome-wide association studies and a linkage analysis identify HERC2 as a human iris color gene [published correction appears in Am J Human Genet 2008;82:801] Am J Hum Genet 2008;82:411−23.

Lango Allen H, Estrada K, Lettre G, Berndt SI, Weedon MN, Rivadeneira F, et al. Hundreds of variants clustered in genomic loci and biological pathways affect human height. Nature 2010;467:832−8.

Marchini J, Howie B, Myers S, McVean G, Donnelly P. A new multipoint method for genome-wide association studies by imputation of genotypes. Nat Genet 2007;39:906−13.

Pruim RJ, Welch RP, Sanna S, Teslovich TM, Chines PS, Gliedt TP, et al. LocusZoom: regional visualization of genome-wide association scan results. Bioinformatics 2010;26:2336−7.

Purcell S, Neale B, Todd-Brown K, Thomas L, Ferreira MA, Bender D, et al. PLINK: a tool set for whole-genome association and population-based linkage analyses. Am J Hum Genet 2007;81:559−75.

Small KS, Hedman AK, Grundberg E, Nica AC, Thorleifsson G, Kong A, et al. Identification of an imprinted master trans regulator at the KLF14 locus related to multiple metabolic phenotypes [published correction appears in Nat Genet 2011;43:1040] Nat Genet 2011;43:561−4.

Wu S, Zhang M, Yang X, Peng F, Zhang J, Tan J, et al. Genome-wide association studies and CRISPR/Cas9-mediated gene editing identify regulatory variants influencing eyebrow thickness in humans. PLoS Genet 2018;14:e1007640.

Yang J, Lee SH, Goddard ME, Visscher PM. GCTA: a tool for genome-wide complex trait analysis. Am J Hum Genet 2011;88:76−82.

Zhou X, Stephens M. Genome-wide efficient mixed-model analysis for association studies. Nat Genet 2012;44:821−4.

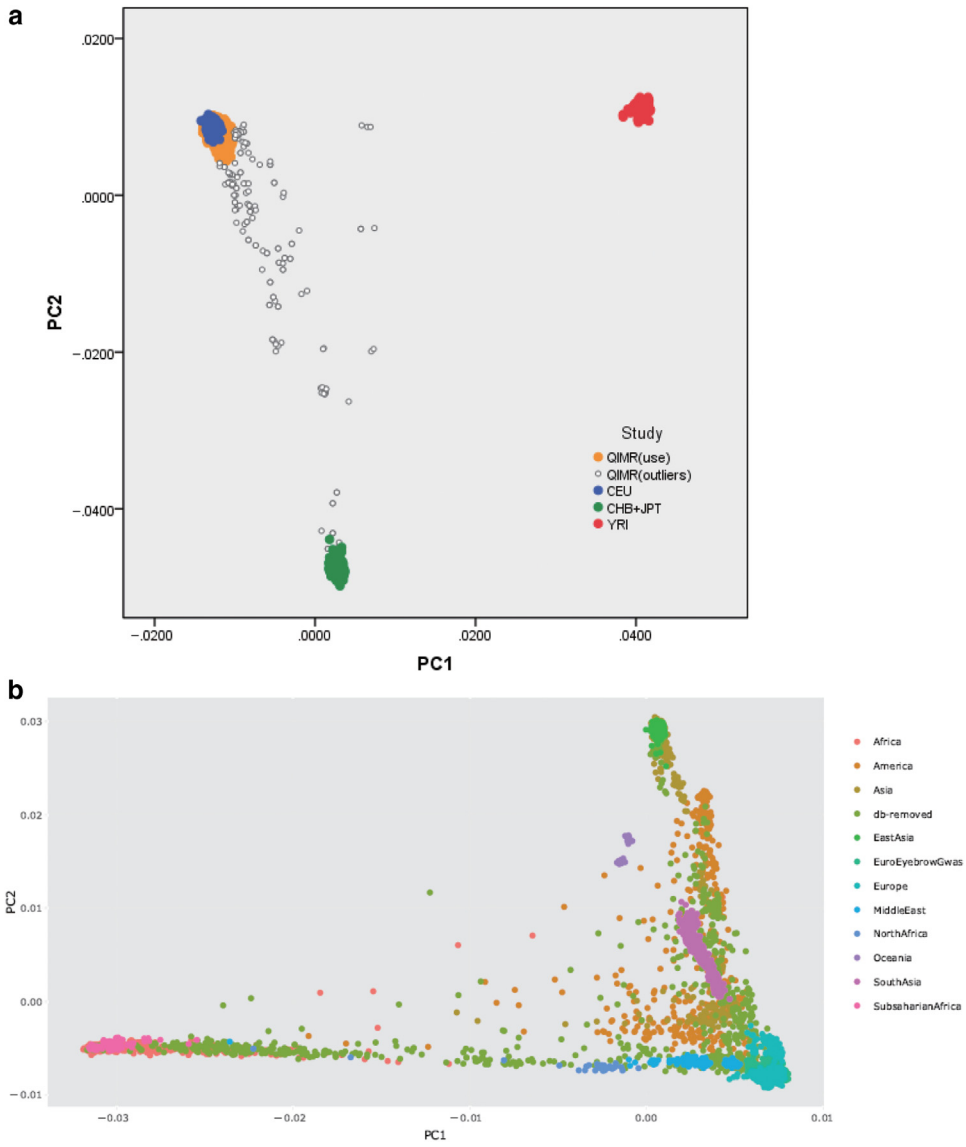

Supplementary Figure S1. PCA of QIMR and US population structure. (**a**) Ancestry of the QIMR samples with respect to three HapMap phase 2 reference population data. Blue circles represent the HapMap European (denoted as CEU) samples, green circles are the HapMap East Asian (denoted as CHB+JPT) samples, and red circles represent the HapMap West African (denoted as YRI) samples. Orange and white circles are samples from QIMR. Samples (white circles) outside of six SDs of the principal component of the CEU samples were removed from further the current GWAS. (**b**) Ancestry of the US cohort samples with respect to the 1000 Genomes Project reference population data. PC1, principal component 1; PC2, principal component 2; QIMR, Queensland Institute of Medical Research; US, United States of America.

Supplementary Figure S2. Example images of eyebrow thickness. Eyebrows were classified into three levels, that is, 0, thin; 1, intermediate; and 2, thick. Level 0 (thin) eyebrow does not cover the skin completely, level 1 (intermediate) eyebrow covers the skin but with less heavy density compared with level 2 (thick).

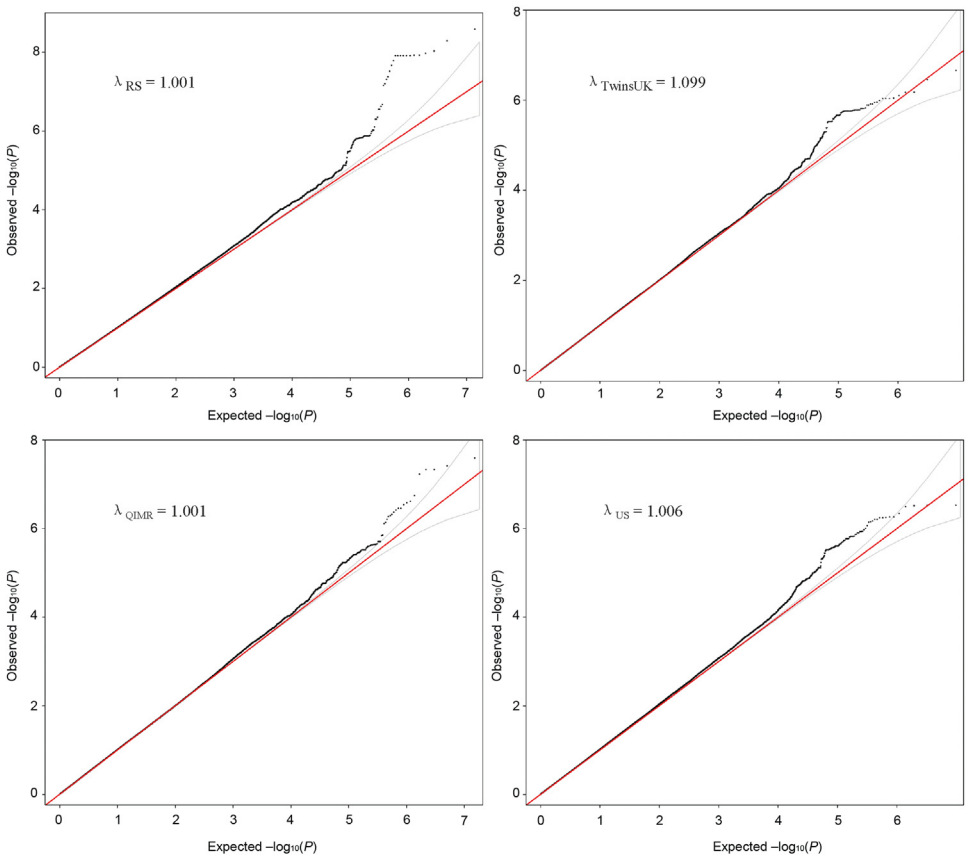

Supplementary Figure S3. Q−Q plots of the eyebrow thickness GWAS results in RS, TwinsUK, QIMR, and US. QIMR, Queensland Institute of Medical Research; RS, Rotterdam Study; US, United States of America.

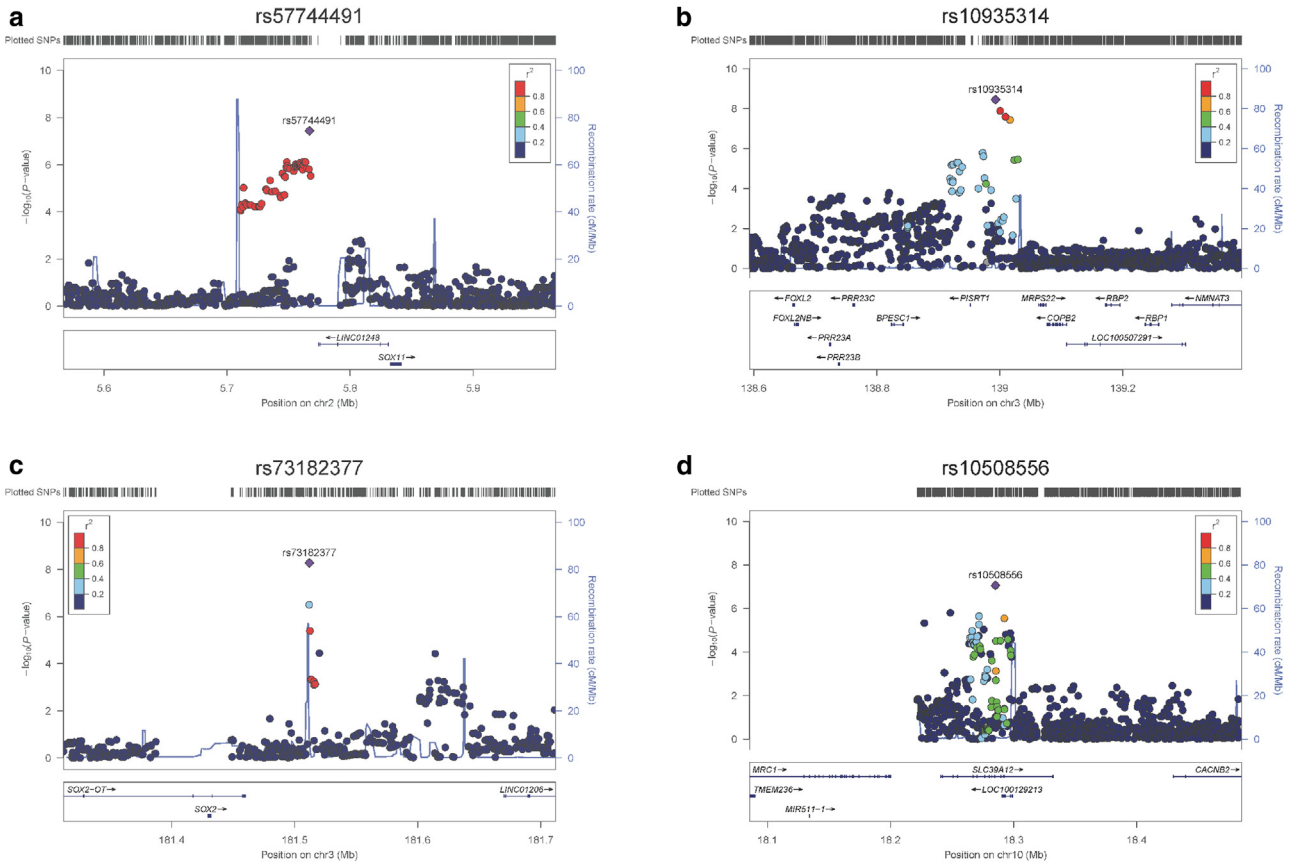

Supplementary Figure S4. Regional Manhattan plots from meta-analysis results. (**a**) 2p25.2-SOX11-rs57744491, (**b**) 3q23-MRPS22-rs10935314, (**c**) 3q26.33-SOX2-rs73182377, and (**d**) 10p12.33-*SLC39A12*-rs10508556.

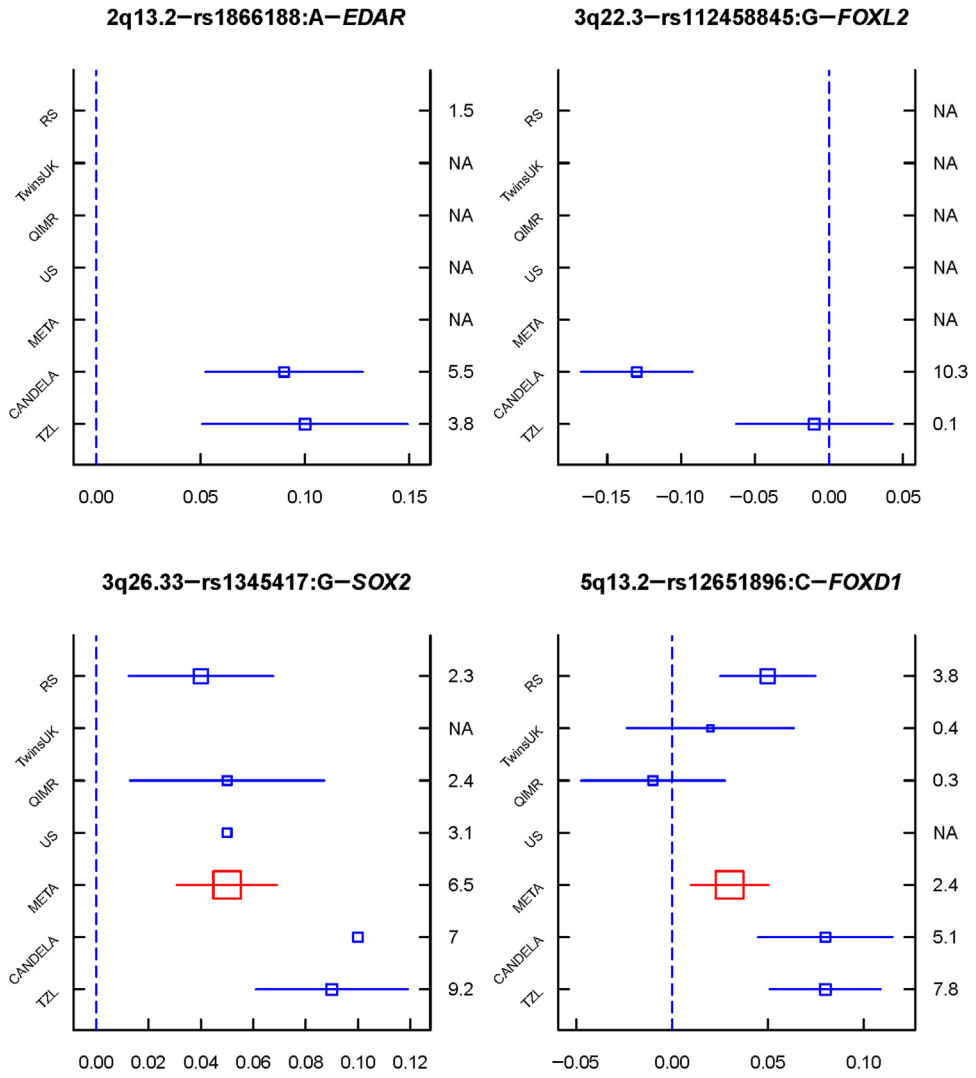

Supplementary Figure S5. Effect sizes for the previously reported lead SNPs in four ET-associated genetic loci (2q13.2-*EDAR*-rs1866188, 3q22.3-FOXL2-rs112458845, 3q26.33-SOX2-rs1345417, and 5q13.2-FOXD1-rs12651896). Blue boxes represent linear regression coefficients (x-axis) estimated in each cohort. Red boxes represent effect sizes estimated in the meta-analyses (denoted as META). Box sizes are proportional to sample size. Horizontal bars indicate a 95% confidence interval of width equal to 1.96 standard errors. The right y-axis indicates *P*-values in each cohort on $-\log_{10}$ scale. ET, eyebrow thickness; NA, not available; QIMR, Queensland Institute of Medical Research; RS, Rotterdam Study; TZL, Taizhou longitudinal study; US, United States of America.

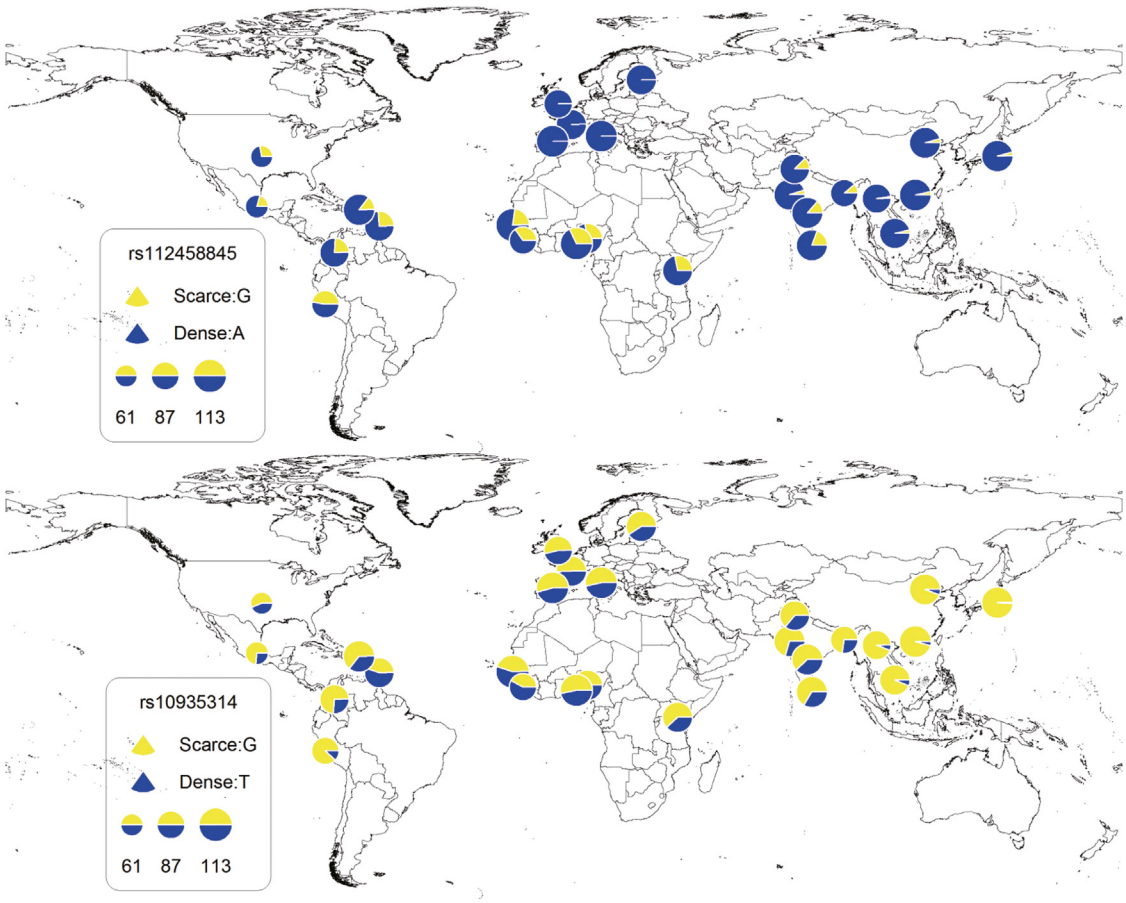

Supplementary Figure S6. Effect allele frequencies of the newly identified SNPs (CANDELA-rs112458845, European-rs10935314) in 26 populations from the 1000-Genomes Project.

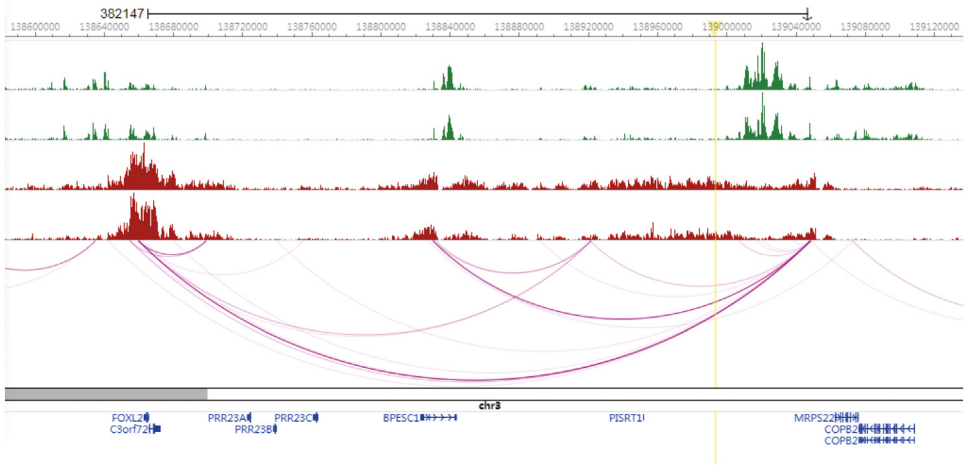

Supplementary Figure S7. ChIA-PET indicates long-range chromatin interaction and suggests the presence of putative regulatory regions at loci associated with eyebrow thickness. The region exhibits distinct active enhancer signatures defined by epigenetic marks, such as H3K4me1 (green) and H3K27me3 (red) histone modifications, on the basis of two independent biological replicates. The position of rs10935314 is indicated by a yellow line. The different tracks were overlaid with physical positions using the WashU Epigenome Browser. ChIA-PET, chromatin interaction analysis with paired-end tag.

Supplementary Table S1. Sample Characteristics

Characteristics	RS (n = 4,411)		TwinsUK (n = 1,159)		QIMR (n = 2,257)		US (n = 2,121)	
Female (n, %)	2,410	55.11	1,159	100.00	1,335	53.90	1,456	68.65
Male (n, %)	2,001	44.89	0	0.00	1,069	46.10	665	31.35
Age (mean, SD)	68.92	9.51	59.73	9.43	16.43	0.80	26.00	11.68
Eyebrow density (n, %)								
Scarce	2,106	48.16	739	63.76	582	23.51	343	16.17
Normal	1,894	43.31	370	31.92	1,258	50.81	1,677	79.07
Dense	373	8.53	50	4.31	636	25.69	101	4.76

Abbreviations: QIMR, Queensland Institute of Medical Research; RS, Rotterdam Study; US, United States of America.
The three levels of eyebrow thickness were rounded from the average score of evaluators.

Supplementary Table S2. Phenotyping Concordance between Evaluators

RS (n = 4,411)				TwinsUK (n = 1,159)				QIMR (n = 2,257)					US (n = 2,121)			
	Rater 1	Rater 2	Rater 3		Rater 1	Rater 2	Rater 3		Rater 1	Rater 2	Rater 3	Rater 4		Rater 1	Rater 2	Rater 3
Rater 1		0.69	0.76	Rater 1		0.68	0.70	Rater 1		0.73	0.73	0.75	Rater 1		0.51	0.54
Rater 2	0.48		0.68	Rater 2	0.52		0.73	Rater 2	0.59		0.71	0.74	Rater 2	0.34		0.56
Rater 3	0.66	0.49		Rater 3	0.61	0.57		Rater 3	0.61	0.57		0.73	Rater 3	0.39	0.42	
Rater 4								Rater 4	0.62	0.59	0.60					

Abbreviations: QIMR, Queensland Institute of Medical Research; RS, Rotterdam Study; US, United States of America.
Values in the upper triangle represent Pearson's correlations and the ones in the lower triangle represent Kappa's test statistics. RS, TwinsUK, and QIMR were phenotyped by the same rater, and the US was phenotyped by another three raters.

Supplementary Table S3. Association Test between Eyebrow Thickness and Sex, Age, and Eyebrow Color

	RS		TwinsUK		QIMR		US	
Characteristics	β	*P*-Value	β	*P*-Value	β	*P*-Value	β	*P*-Value
Sex (female)	−0.38	########	/	/	−0.33	2.78E-50	−0.23	#######
Age	−0.01	1.33E-10	−0.01	3.60E-13	0.02	1.40E-01	−0.01	#######
Eyebrow color	0.30	1.57E-59	0.44	4.65E-34	0.31	7.66E-79	0.06	#######

Abbreviations: QIMR, Queensland Institute of Medical Research; RS, Rotterdam Study; US, United States of America.

Supplementary Table S4. Heritability Estimation Using ACE and ADE Models in QIMR Dataset

Model	A	C | D	E	-2LL	df	Comp.	ΔX^2	*P*-Value
ACE	82.69 (77.28–85.06)	0 (0–4.86)	17.31 (14.94–20.13)	3586.7	2470			
AE	82.69 (79.87–85.06)	—	17.31 (14.94–20.13)	3586.7	2471	2 versus 1	0	1.00E+00
CE	—	54.07 (49.82–58.03)	45.93 (41.97–50.18)	3793.3	2471	3 versus 1	206.5	7.78E-47
ADE	57.31 (30.57–82.55)	25.41 (0.27–52.49)	17.07 (14.79–19.78)	3582.8	2470			
AE	82.69 (79.87–85.06)	—	17.31 (14.94–20.13)	3586.7	2471	5 versus 4	3.9	4.70E-02

Abbreviation: A, *additive* genetic effects; C, common (or shared) environmental effects; D, non-additive genetic (or *dominance*) effects; E, specific (or nonshared) *environment* effects plus measurement error; Comp., comparison; df, difference; QIMR, Queensland Institute of Medical Research.

Supplementary Table S5. Lead SNPs for Meta-Analysis Results for Four European Cohorts (n = 9,948)

							META (n = 9,948)	
SNP	CHR	BP	Locus	Gene	EA	OA	β	*P*-Value
rs57744491	2	5766939	2p25.2	*SOX11*	G	A	−0.11	#######
rs10935314	3	1.39E+08	3q23	*MRPS22*	T	G	0.05	#######
rs73182377	3	1.82E+08	3q26.33	*SOX2*	T	C	0.05	#######
rs10508556	10	18285342	10p12.33	*SLC39A12*	T	C	0.04	#######

Abbreviations: BP, base position; CHR, chromosome; EA, effect allele; fEA, frequency of the effect allele; META, meta-analysis; QIMR, Queensland Institute of Medical Research; RS, Rotterdam Study; US, United States of America.
META denotes META RS, TwinsUK, QIMR, and US GWASs results.

Supplementary Table S6. GWASs and Meta-Analysis Results for Four European Cohorts (n = 9,948)

				RS (n = 4,411)			TwinsUK (n = 1,159)			QIMR (n = 2,257)			US (n = 2,121)			META (n = 9,948)		CANDELA (n = 2,457)			TZL (n = 2,961)		
SNP	**CHR**	**BP**	**EA**	**fEA**	**β**	***P*-Value**	**fEA**	**β**	***P*-Value**	**fEA**	**β**	***P*-Value**	**fEA**	**β**	***P*-Value**	**β**	***P*-Value**	**fEA**	**β**	***P*-Value**	**fEA**	**β**	***P*-Value**
rs57744491	**2**	**5766939**	**G**	**0.05**	**−0.11**	**1.71E-05**	**NA**	**NA**	**NA**	**NA**	**NA**	**NA**	**0.05**	**−0.11**	**5.81E-04**	**−0.11**	**3.60E-08**	**0.09**	**−0.02**	**4.87E-01**	**0.22**	**−0.01**	**4.10E-01**
rs1866188	2	109257152	A	NA	NA	NA	NA	NA	NA	NA	NA	NA	NA	NA	NA	NA	NA	0.40	0.09	3.54E-06	0.92	0.10	1.46E-04
rs112458845	3	138675741	G	NA	NA	NA	NA	NA	NA	NA	NA	NA	NA	NA	NA	NA	NA	0.27	−0.13	4.95E-11	0.07	−0.01	7.30E-01
rs10935314	**3**	**138993138**	**T**	**0.44**	**0.06**	**4.93E-08**	**NA**	**NA**	**NA**	**0.45**	**0.04**	**4.54E-02**	**0.46**	**0.03**	**2.59E-02**	**0.05**	**3.51E-09**	**0.26**	**0.04**	**6.01E-02**	**0.05**	**−0.02**	**4.45E-01**
rs4894342	3	139000844	T	0.43	0.06	2.42E-07	NA	NA	NA	0.45	0.04	3.14E-02	0.45	0.03	3.78E-02	0.04	1.27E-08	0.23	0.03	1.15E-01	0.03	0.01	7.37E-01
rs2046965	3	139009532	T	0.43	0.06	2.15E-08	NA	NA	NA	0.45	0.03	8.85E-02	0.45	0.02	8.70E-02	0.04	2.54E-08	0.24	0.03	2.13E-01	0.42	0.02	1.72E-01
rs4438684	3	139016767	T	0.43	0.06	4.22E-08	NA	NA	NA	0.45	0.03	9.82E-02	NA	NA	NA	0.05	3.63E-08	0.23	0.02	3.19E-01	0.43	0.02	1.60E-01
rs1345417	3	181511951	G	0.57	0.04	5.45E-03	NA	NA	NA	0.60	0.05	3.62E-03	0.61	0.05	7.30E-04	0.05	3.13E-07	0.52	0.10	1.04E-07	0.27	0.09	6.51E-10
rs73182377	**3**	**181512034**	**T**	**0.23**	**0.04**	**3.61E-03**	**0.21**	**0.09**	**3.68E-04**	**0.23**	**0.03**	**1.38E-01**	**0.26**	**0.05**	**4.08E-04**	**0.05**	**5.25E-09**	**0.16**	**0.08**	**6.02E-04**	**0.10**	**0.12**	**2.25E-07**
rs12651896	5	72502029	C	0.28	0.05	1.62E-04	0.29	0.02	3.85E-01	0.31	-0.01	5.41E-01	NA	NA	NA	0.03	3.65E-03	0.32	0.08	7.54E-06	0.27	0.08	1.73E-08
rs10508556	**10**	**18285342**	**T**	**0.47**	**0.03**	**2.89E-02**	**0.46**	**0.02**	**2.88E-01**	**0.48**	**0.07**	**1.03E-05**	**0.46**	**0.04**	**1.53E-03**	**0.04**	**3.19E-08**	**0.63**	**0.03**	**7.47E-02**	**0.73**	**0.01**	**5.05E-01**

Abbreviations: BP, base position; CHR, chromosome; EA, effect allele; fEA, frequency of the effect allele; META, meta-analysis; NA, not applicable; QIMR, Queensland Institute of Medical Research; RS, Rotterdam Study; US, United States of America.

META denotes the META of RS, TwinsUK, QIMR, and US GWASs results. The *P*-values of the genome-wide significant SNPs in META were marked in red color. The four lead SNP at each locus identified in European origin meta-analysis were highlighted in bold. The four SNPs reported previously (Adhikari et al., 2016; Wu et al., 2018) were also included in this table (can be identified from *P*-values without color in META results).

Supplementary Table S7. QC Thresholds for Each Cohort

Cohorts	INFO	LD R2	MAF	SNP-Wise Call Rate	Individual Call Rate	HWE	IBD
RS	0.80	—	0.05	0.97	0.97	1.00E-04	0.2
TwinsUK	0.80	—	0.05	0.97	0.97	1.00E-04	0.2
QIMR	—	0.70	0.01	0.95	0.95	1.00E-06	0.2
US	0.30	—	0.025	0.90	0.90	1.00E-06	0.19

Abbreviations: IBD, identity by descent; INFO, information score reported by IMPUTE; HWE, Hardy–Weinberg equilibrium; LD, linkage disequilibrium; MAF, minor allele frequency; QC, quality control; QIMR, Queensland Institute of Medical Research; RS, Rotterdam Study; US, United States of America. INFO was produced by IMPUTE; LD R2 was produced by SHAPEIT/minimac pipeline.

Supplementary Table S8. Phenotypic Variance of Eyebrow Thickness in European Populations

Cohorts	All Sample	Male	Female
RS	0.34	0.39	0.24
TwinsUK	0.26	NA	0.26
QIMR	0.35	0.38	0.27
US	0.20	0.23	0.16

Abbreviations: NA, not applicable; QIMR, Queensland Institute of Medical Research; RS, Rotterdam Study; US, United States of America.

Supplementary Table S9. Sex-Stratification Analysis of the Lead SNPs Associated with Eyebrow Thickness Reported in this Study and Previous Studies

				Male		Female	
SNP	CHR	BP	EA	β	*P*-Value	β	*P*-Value
rs57744491	2	5766939	G	−0.19	5.82E-06	−0.04	2.13E-01
rs10935314	3	138993138	T	0.11	1.52E-08	0.03	5.65E-02
rs4894342	3	139000844	T	0.11	4.02E-08	0.02	1.01E-01
rs2046965	3	139009532	T	0.12	3.04E-09	0.02	7.95E-02
rs4438684	3	139016767	T	0.11	1.24E-08	0.02	6.77E-02
rs1345417	3	181511951	G	0.03	1.72E-01	0.05	5.72E-03
rs73182377	3	181512034	T	0.07	6.02E-03	0.02	2.27E-01
rs12651896	5	72502029	C	0.08	2.85E-04	0.02	1.45E-01
rs10508556	10	18285342	T	0.05	7.41E-03	0.00	7.44E-01

Abbreviations: BP, base position; CHR, chromosome; EA, effect allele.